PERSPECTIVE ARTICLE

Comprehensive peri-implant tissue evaluation with ultrasonography and cone-beam computed tomography: A pilot study

Rafael Siqueira[1] | Khaled Sinjab[1] | Ying-Chun Pan[2] | Fabiana Soki[3] | Hsun-Liang Chan[1] | Oliver Kripfgans[2,4]

[1]Department of Periodontics and Oral Medicine, University of Michigan School of Dentistry, Ann Arbor, MI, USA

[2]Department of Biomedical Engineering, College of Engineering, Ann Arbor, MI, USA

[3]Department of Periodontics and Oral Medicine and Division of Oral Pathology/ Medicine/Radiology, University of Michigan School of Dentistry, Ann Arbor, MI, USA

[4]Department of Radiology, University of Michigan Medical School, Ann Arbor, MI, USA

Correspondence
Hsun-Liang Chan, DDS, MS, Clinical Associate Professor of Dentistry, Assistant Program Director, Periodontics Graduate Program, Department of Periodontics and Oral Medicine, University of Michigan School of Dentistry, 1011 North University Avenue, Ann Arbor, Michigan 48109-1078, USA.
Email: hlchan@umich.edu

Abstract

Objectives: The aim of the present study was to explore the feasibility of ultrasonography (US) for clinical imaging of peri-implant tissues.

Material and Methods: Patients with ≥1 implant, a cone-beam computed tomography (CBCT) scan, an US scan, and clinical photographs taken during the surgery were included. The crestal bone thickness (CBT) and facial bone level (FBL) were measured on both US and CBCT modalities, and direct FBL measurements were also made on clinical images. US measurements were compared with CBCT and direct readings.

Results: A total of eight implants from four patients were included. For FBL measurements, US and direct (r2 = 0.95) as well as US and CBCT (r2 = 0.85) were highly correlated, whereas CBCT correlated satisfactorily with the direct reading (r2 = 0.75). In one implant without facial bone, CBCT was not able to measure CBT and FBL accurately. The estimated bias for CBT readings was 0.17 ± 0.23 mm (p = .10) between US and CBCT. US blood flow imaging was successfully recorded and showed a wide dynamic range among patients with different degrees of clinical inflammation.

Conclusion: US is a feasible method to evaluate peri-implant facial crestal bone dimensions. Additional US features, for example, functional blood flow imaging, may be useful to estimate the extent and severity of inflammation.

KEYWORDS
alveolar bone, artifacts, cone-beam computed tomography, dental implants, imaging, peri-implantitis, soft tissue, ultrasonography

---

Rafael Siqueira and Khaled Sinjab equally contributed to this study

----

1 | INTRODUCTION

Despite the high survival rate of dental implants reported in long-term studies (Adler et al., 2020; Moraschini et al., 2015), biological complications have started to surface at a rapid pace in the literature (Berglundh et al., 2018). To emphasize this imminent problem, the American Academy of Periodontology/European Federation of Periodontology World Workshop proposed a peri-implant disease classification (Renvert et al., 2018). Peri-implant mucositis is characterized by tissue inflammation without pathological bone loss; peri-implantitis presents with progressive bone loss (Renvert et al., 2018). The other category is peri-implant tissue deficiencies, featuring deficient hard and soft peri-implant tissue without overt inflammation. As is true in medicine, accurate and comprehensive diagnosis of peri-implant diseases is the key leading to precise treatment and optimal outcomes. In addition to clinical examinations, various intraoral and extraoral radiographs have been applied to aid in accurate evaluation of peri-implant hard tissue (Rios et al., 2017).

Intraoral radiographs are the current gold standard to evaluate implant marginal bone level, which is the primary measure of peri-implantitis (Berglundh et al., 2018). While adequate to present the superimposed interproximal bone level, they are not able to image the facial and lingual/palatal bone. Normal bone remodeling and pathologic loss due to disease activity are not symmetrical around implants (Monje, Pons, et al., 2019; Schwarz et al., 2007). Other than the marginal bone level, facial bone thickness bears clinical implications and should be evaluated prudently. It is correlated with the periodontal phenotype, facial ridge contour, mucosal level and the risk for mucosal recession (Fu et al., 2010; Monje, Chappuis, et al., 2019; Spray et al., 2000). Therefore, to fully assess peri-implant bone dimensions, a cross-sectional imaging modality is necessary. Currently, the only established non-invasive, cross-sectional imaging for these purposes is cone-beam computed tomography (CBCT) (Chan et al., 2010). It functions by emitting cone-shaped radiation when revolving around a patient. The transmitted radiation is then received on the other side by a detector and processed into 3-dimensional (3-D) images using a computer algorithm.

In the literature, CBCT has been widely used for research and clinical patient care because of its versatile applications (Horner et al., 2015; Jacobs et al., 2018). Although CBCT can provide 3-D images of peri-implant tissues, one of the greatest limitations is the inherent artifacts surrounding high-density materials such as metallic restorations and implants that degrade image quality and interfere with image interpretation. When the bone is thin or the possibility of fenestration or dehiscence is considered, the negative impact arising from artifacts is more significant (de-Azevedo-Vaz et al., 2016; Peterson et al., 2018). Unfortunately, these are the critical clinical scenarios where high-resolution imaging is desperately required to assist in clinical decision-making. Additionally, while suitable for hard-tissue imaging, CBCT has poor dynamic range for soft-tissue imaging and is not intended for soft-tissue assessment (Bornstein et al., 2014; Tyndall et al., 2012). Functional soft-tissue evaluation, for example, evaluation of blood flow/volume and tissue content is not provided by CBCT.

Ultrasound (US) is another cross-sectional imaging modality with an additional benefit of non-ionizing radiation. Other advantages include real-time (point-of-care), portability and cost efficiency as well as direct interaction of the examiner with the patient (Dietrich et al., 2019). Technological advances have allowed for manufacturing of high-resolution and miniature-sized probes suitable for superficial tissue imaging in dermatology, etc. In dentistry, the same device specifications are required. Recent cadaverous proof-of-principle study (Chan et al., 2018) demonstrated the accuracy of the US in imaging peri-implant hard and soft tissues. US provides superior soft-tissue images with a wide dynamic range and a clear delineation of hard-tissue surfaces (Chan & Kripfgans, 2020). Therefore, it can be used in combination with CBCT to examine peri-implant tissues to mitigate the potential errors arising from artifacts associated with CBCT imaging on implants. The primary aim of this retrospective pilot study was to evaluate the feasibility of US to image facial peri-implant tissues in live humans and narratively highlight additional benefits of US for a comprehensive examination of peri-implant tissues. The hypothesis is that US measurements present agreement with CBCT and direct measurements in a way it can be utilized as a supplementary tool to evaluate peri-implant tissue dimensions.

2 | MATERIALS AND METHODS

This study was approved by the University of Michigan Institutional Review Board (IRB) with a registration number HUM00179671. Description of this observational study complied with the appropriate EQUATOR guidelines. A chart review was conducted between November 2019 and February 2020 to identify qualified clinical cases registered in the Graduate Periodontal Clinic at University of Michigan School of Dentistry. To be included, the patients had to have ≥1 implant with a CBCT scan, US scan, and clinical photographs taken during the surgery, for example, a revision/implant removal surgery due to peri-implantitis or a 2nd-stage uncovery surgery. The photographs taken during the surgery allow for the ground truth examination, that is, crestal bone level. In addition, the CBCT and US images had to be taken within 3 months from when the photographs were taken.

2.1 | Ultrasound scans and measurements

The US scans were off-label used to non-invasively evaluate peri-implant bone and soft-tissue dimensions before the planned surgery. The scanning protocol was described in detail in a recent publication (Chan & Kripfgans, 2020). Briefly, a commercially available US imaging device (ZS3, Mindray, Mountain View CA, USA) coupled with a toothbrush-sized (~30 × 18 × 12 mm) and high-resolution (24 MHz, 64 μm axial image resolution) probe was used (Figure 1). Both the B- and color-flow modes were used for imaging. B-mode images allowed for visualization and quantification of spatial relations, including soft–hard tissue boundaries, implant structures

FIGURE 1 Clinical picture of the US probe, toothbrush-sized (~30 × 18 × 12 mm), used in the study allowing scan of an implant in between adjacent teeth

and soft-tissue characterization as a result of backscatter changes in real-time. On the image, the implant platform typically showed a bright (hyperechoic) white solid line, whereas the threads were best described as a dash line, with continuous bright and dark short lines corresponding to the peaks and valleys of the threads, respectively (Figure 2). Blood flow direction and relative velocity were imaged with the color-flow mode. The red and blue colors were assigned to image pixels depending on the flow direction and velocity in a particular voxel. The color pixel intensity in a given region of interest (ROI) was hypothesized to correlate with the degree of blood perfusion and thus may indicate inflammatory severity. To image the mid-facial site of the studied implants using US, the probe was first positioned in mesio-distal direction and moved apico-coronally by freehand to identify the most prominent point of the implant platform. This was made possible because US images were displayed in real-time on a 15-inch computer monitor while scanning. Once this site was visualized, then the probe was turned in apico-coronal direction until it aligned with the implant long axis. In this position, the image brightness of the implant was the strongest because most of the sound reflected directly and received by the same probe. B-mode and color-flow images were stored in Digital Imaging and Communications in Medicine (DICOM) format. On the B-mode image, two parameters, the crestal bone thickness (CBT) and the facial bone level (FBL), were measured by a calibrated examiner with 5 years of dental ultrasound experience (HC). CBT was measured at 1 mm apical to the bone crest. FBL, also known as the exposed implant length, was measured from the implant platform to the bone crest. Color-flow images were narratively described.

2.2 | CBCT images and measurements

The CBCT scan was prescribed as a part of clinical care to assess peri-implant bone dimension before the planned surgery. These scans were taken at the University of Michigan School of Dentistry using a commercially available CBCT scanner (3D Accuitomo 170; J Morita, Kyoto, Japan). The settings for exposure were 5 mA and 90 kVp for 17.5 s. The field of view (FOV) was set at 140*100 mm and the voxel size at 0.27 mm. Images were then converted into DICOM files that were later imported into a commercially available software package for CBCT measurements (Anatomage Invivo 6, © 2018 Anatomage Inc) and further analysis. A mid-facial cross-sectional image was selected according to the orientation of the US image. Knowing CBCT and US images were not co-registered, 2 more cross-sectional CBCT images were selected at 1 mm from the mid-facial image on both mesial and distal sides. On these 3 slices, CBT and FBL were measured by an oral maxillofacial radiologist (FS) with >3 years of experience. Feasibility of US to estimate CBT and FBL was evaluated by the range of the measurements made on the 3 CBCT slices.

2.3 | Direct measurements

Direct measurements of FBL were estimated using a proprietary programming language (MATLAB, Natick, Massachusetts, USA). An example of such measurements was provided in S Figure S1. Briefly, the implant platform and threads were modeled as a circle and spiral, respectively in 3D. These features were collectively calibrated and rotated about the x-, y- and z-axis until the x and y coordinates fit the corresponding features in the image. The scaling factor, the true diameter of the implant platform, thread pitch distance and angles of rotation were used to estimate FBL.

2.4 | Statistical analysis

Anatomical structures of peri-implant tissues on B-mode US images in relation to CBCT and direct measurements were narratively described. Features of color-flow images were also described. The overall agreements in FBL and CBT between the three methods were evaluated by bar plots. In addition, correlation plots for FBL were made between US, CBCT and clinical measurements. The squared correlation coefficient values (R^2) were calculated. A Bland–Altman plot was used to estimate the bias of CBT measurements between US and CBCT.

3 | RESULTS

A total of eight implants from four patients were available. Representative images of the mid-facial site of the implants on cross-sectional CBCT images, US B-mode and color images, and direct assessment were shown in Figure 2 (Implants 1–4) and Figure S2 (Implants 5–8). B-mode US images demarcated the bone crest, and the facial bone (FB) as a curved bright white line (hyperechoic) well. The facial mucosa (FM) shown on the B-mode image was visualized by the US and represented by different intensities that may
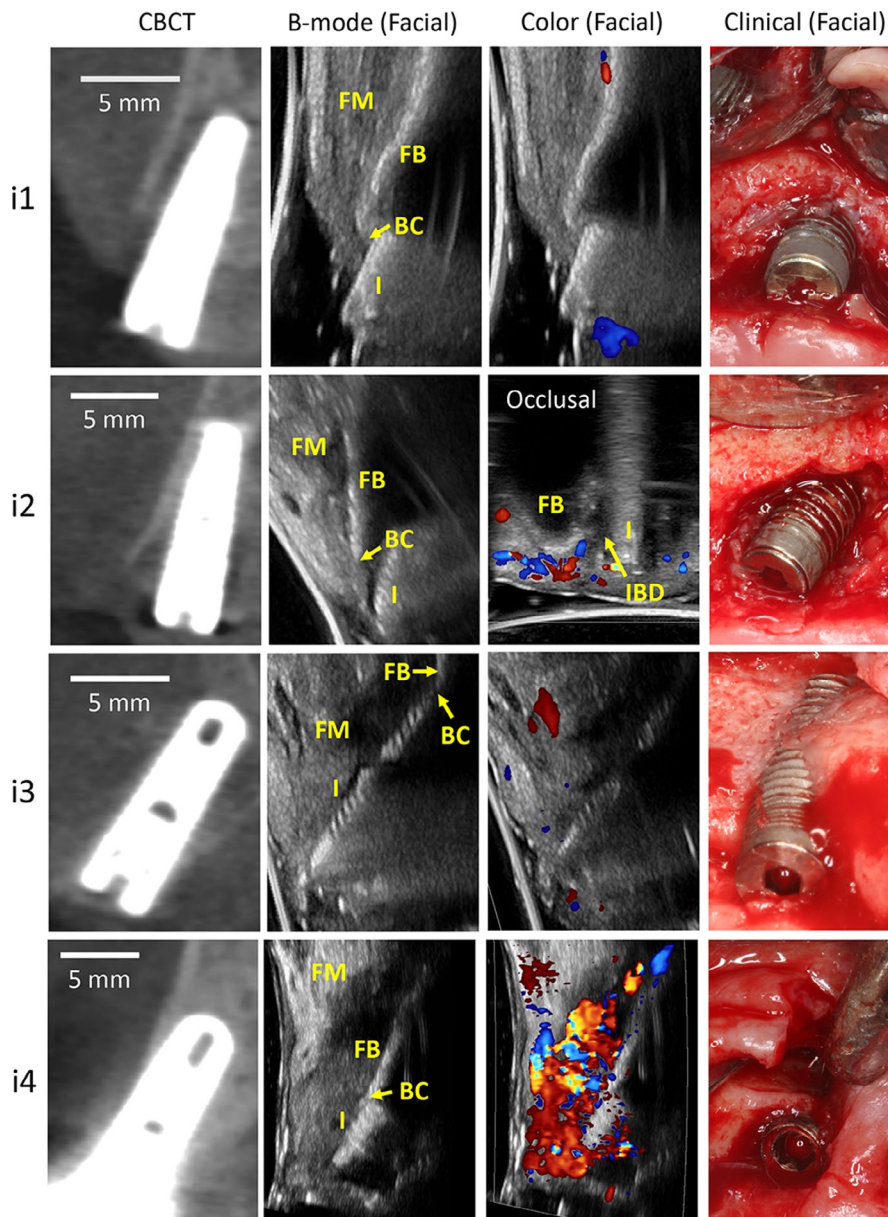
FIGURE 2 Representative images of Implants 1–4 (i1-i4) examined with CBCT, US in B-mode and Color-mode, and a clinical photograph. The cross-sectional B-mode US clearly demarcated the exposed implant surface (I), evidenced by the presence of threads, the bone crest (BC), the facial bone (FB) and the facial mucosa (FM). Soft-tissue image and blood flow are visualized in the color mode US image information. (FM=facial mucosa; FB=facial bone; BC=bone crest; I=exposed implant surface)

suggest different tissue textures, composition and inflammation status. When the facial crestal bone was thicker, both CBCT and US could delineate the peri-implant bone (Figure 2 i1 and i2). For examples for Implant 1 (Helix GM Acqua, Neodent, Curitiba, Brazil), both CBCT and US images showed the FBL and CBT coincided with each other and their clinical appearances. However, when there was thinner facial bone or in cases of completely exposed implants, beam hardening and volume averaging artifacts on CBCT images hindered the assessment of the implant surroundings, especially in cases of dehiscence or fenestrations (Figure 2 i3 and i4). On the US B-mode image of Figure 2 i3, the implant surface (I), characterized by implant threads devoid of facial bone coverage, was still delineated. Additionally, the US can demarcate an infrabony defect (IBD), which was also confirmed on CBCT and the clinical photograph (Figure 2 i2).

Color-mode US images in Figure 2 showing colored pixels in red and blue represented blood flow within the soft tissue. There was minimal blood flow noted in the soft tissue of implants 1–3, suggestive of minimal inflammation (Figure 2 i1-3). On the other hand, the color mode of implant 4 (Figure 2 i4) showed significantly elevated numbers and intensity of color pixels, indicating a marked increase in blood flow to the area which suggests increased inflammation.

Figure 3a showed a range plot comparing FBL from the three methods. US readings in general fell into the ranges of CBCT or direct assessments collected from the mid-facial site, and 1 mm mesial and distal to the mid-facial sites. Of special notice was implant #3, which had bony dehiscence in its full length. US was able to identify this large dehiscence but not CBCT. Figure 3b demonstrates the correlation of the FBL between US, CT and direct measurements. Implant 3 (red point) was considered an outlier and was not included within the best-fit line because CBCT underestimated FBL. Overall, US had a high correlation with direct measurements (slope = 0.93, bias = 0.35 mm, $r2 = 0.95$) and with CBCT (slope = 0.84, bias = 0.61 mm, $r2 = 0.82$). CBCT had a satisfactory correlation with

FIGURE 3 (a) A bar chart showing FBL comparisons between CBCT, US and direct measurements across all eight implants, sorted by the mean direct measurement. (b) FBL correlations between US, CT and direct measurements. The best-fit line was drawn with the seven blue points, while the red point was an outlier corresponding to i3. The 95% confidence intervals were included in the parenthesis
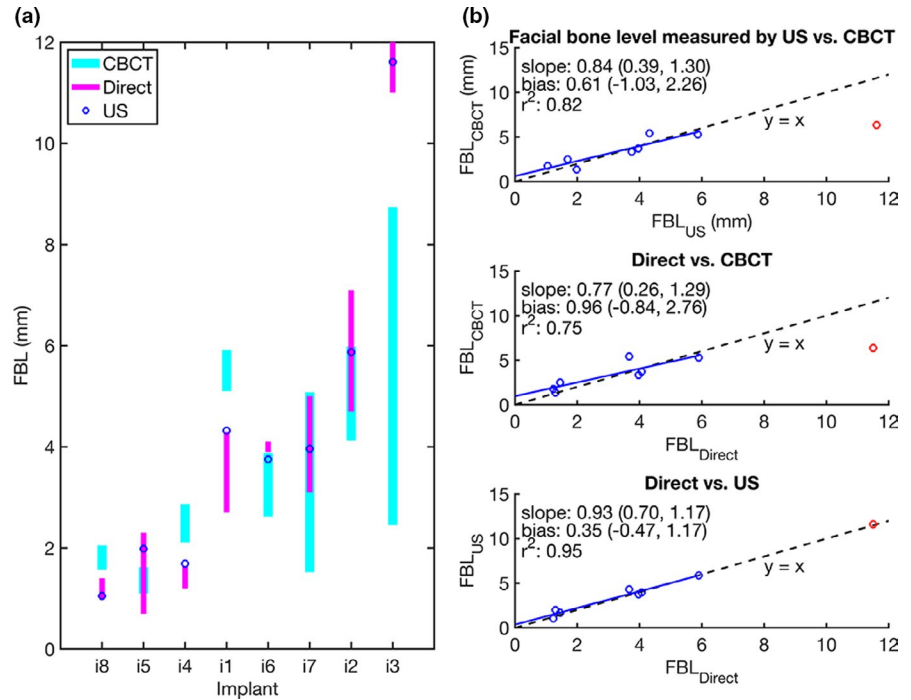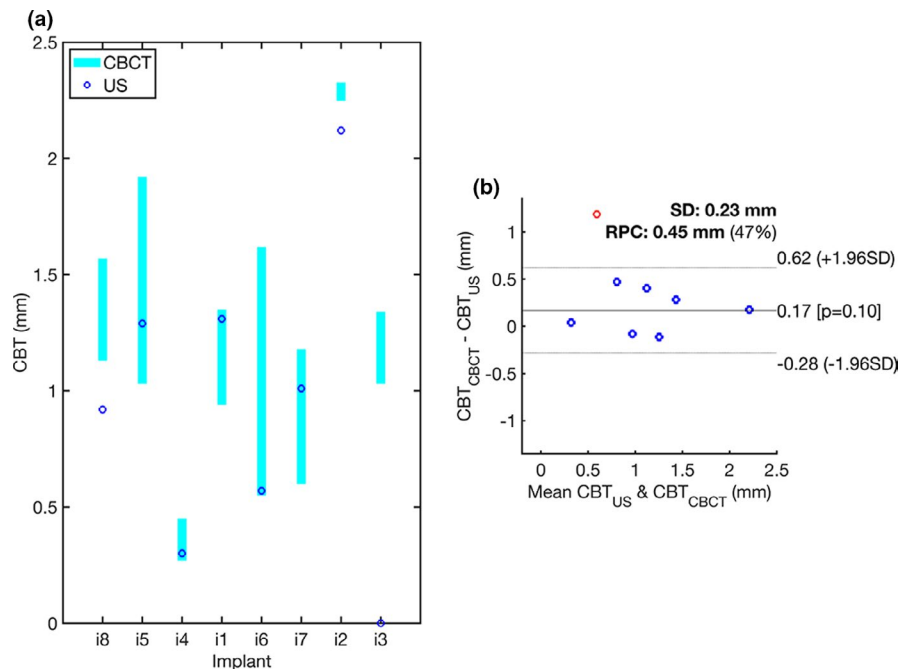

FIGURE 4 (a) A bar chart of CBCT- and US-based CBT sorted by the mean direct measurement. (b) Bland–Altman plot of CBT measurements using CBCT and US. The estimated bias was 0.17 mm ($p = .10$), while the reproducibility coefficient (RPC, $1.96 * SD$) was 47% of the mean CBT measurement across both modalities. The red point, corresponding to implant 3, was excluded from the analysis

direct measurements (slope = 0.77, bias = 0.96 mm, and r2 = 0.75). In summary, Figure 3 suggests that CBCT accuracy is affected in the presence of thin crestal bone resulting in potential misdiagnose of FBL while US scans aided in the FBL evaluation and mitigated the existing artifacts present in the CBCT.

Figure 4a showed a range plot comparing CBT between US and CBCT. Overall, US was comparable to CBCT in estimating CBT. Again, due to the lack of facial bone around implant #3, CBCT could not locate the crestal bone and to determine CBT accurately. Figure 4b presented the CBT differences between the US and CBCT against the means of the US and CBCT (the Bland–Altman Plot). The

estimated bias was 0.17 ± 0.23 mm without statistical significance ($p = .10$), while the reproducibility coefficient (RPC, $1.96 * SD$) was 47% of the mean CBT measurement across both modalities.

4 | DISCUSSION

Emerging evidence indicates CBCT limitations in imaging peri-implant bone are due to the presence of artifacts (Demirturk Kocasarac et al., 2019; Jacobs et al., 2018; Vanderstuyft et al., 2019). They are in the forms of streaks, lines and shadows oriented along the

radiation projection pathway, potentially degrading the image quality as shown in Figure 2. Beam hardening, scatter and photon starvation are common metal-induced artifacts (Pauwels et al., 2013; R. Schulze et al., 2011; R. K. Schulze et al., 2010). Beam hardening artifacts are generated when lower energy X-rays within a polychromatic spectrum are substantially absorbed by the high-density material (i.e., dental implant) resulting in a higher energy beam (hardening of the beam) that is captured by the detector. These errors appear in the image as bright streaks and darkened areas. Photon starvation is part of streak artifacts due to high attenuation of the beam that results in insufficient photons reaching the detectors. Volume averaging artifacts form when the boundary of two objects with different attenuation properties (i.e., an implant and its surrounding bone) are positioned within a voxel. An averaged image grayscale is given to the voxel instead of the actual density, resulting in an inferior delineation of the implant–bone interface. These artifacts add on and subsequently cause either underestimation or overestimation of bone dimensions due to the impaired image quality, which is especially true in thin or absent crestal bone. A recent systematic review concluded that CBCT-based linear measurements may both over- or underestimate peri-implant bone loss and has a lower accuracy for dehiscence defects in in-vitro experiments (Pelekos et al., 2018).

US may be used to complement CBCT when artifacts are found to impair diagnostic values. The results here presented as well as the findings of previous human cadaverous study (Chan et al., 2018) suggest the feasibility and accuracy of US in measuring peri-implant tissues. The bone defect morphology affected by peri-implantitis is very dynamic and is considered a primary factor in deciding the type of surgical treatment. Preliminary data from this study showed feasibility of US to image infrabony defects. In addition, several clinical parameters have been identified as risk indicators for peri-implant diseases, for example, crestal bone thickness, thin phenotype, inadequate width of keratinized mucosa (Linkevicius et al., 2015; Monje, Chappuis, et al., 2019; Perussolo et al., 2018; Schwarz, Becker, et al., 2018; Schwarz et al., 2018; Spray et al., 2000). Information from clinical and preclinical studies suggests that a facial bone plate greater than 1.5 to 2 mm after implant installation might be sufficient to reduce the risk of bony dehiscence during the early phases of postsurgical healing (Monje, Chappuis, et al., 2019; Spray et al., 2000). Also, a more coronally located crestal bone level can possibly lead to less exposure of implant threads and biofilm accumulation on the rough implant surface and, thus, reduce the risk of peri-implantitis (de Siqueira et al., 2020; Vervaeke et al., 2018). Crestal soft-tissue thickness is related to the amount of marginal bone loss.

TABLE 1 Comparison of CBCT and US imaging methods in the mode of mechanism, main functions, image resolution and clinical indications

Imaging features	CBCT	US
Mode of mechanism	Transmission	Reflection
Cross-sectional imaging	Yes	Yes
Anatomical information	Yes	Yes
Functional information, for example, blood flow	No	Yes
Imaging resolution	~150–250 mm	~60 mm
Intrabony information	Yes	No
Bone surface delineation	Fair to good, less reliable when bone is thinner (<= 1 mm)	Fair to good in general
Soft-tissue delineation	Poor	Excellent
Negative Imaging quality around metal objects	Yes	No
Point-of-care	No	Yes
Radiation	Yes	No
Cost	Expensive	Less expensive
Operator dependent	Less	More
Imaging timing	• Most suitable during treatment planning phase • May be performed intraoperatively • Less indicated during maintenance phase due to presence of artifacts around metals	• Most suitable during maintenance phase • Can be used as a quick screening tool before ordering a CBCT scan during treatment planning phase • May be performed intraoperatively with minimally invasive surgery
ROI size	Most suitable for larger area, for example, a few teeth and the whole jaw	Focal area, currently a surface of a tooth or an implant
Peri-implant tissue imaging	Provide general spatial relationship between the implant the surrounding bone, and vital structures	Provide detailed facial bone location, crestal bone thickness, soft-tissue features, muscle attachment and blood flow, etc.

Clinical studies suggested that in the presence of a thick mucosal tissue (frequently reported as >2 mm), stable marginal bone levels and peri-implant health were encountered (van Eekeren et al., 2017; Linkevicius et al., 2009, 2015, 2018; Thoma et al., 2020). The above-mentioned parameters can also be measured on US images making it a useful research and clinical device to monitor peri-implant tissues non-invasively at chairside.

Typically, peri-implantitis appears a few years after an implant is in function; however, hard- and soft-tissue quality and quantity at the planned site may predispose an implant to this disease. Hence, timely and prudent clinical evaluations and imaging acquisition are critical for early identification of risk factors and disease activity. CBCT can be of extremely helpful in the implant treatment planning phase to visualize the available bone volume and to design the implant position before the surgery (Chan et al., 2010). Monitoring the peri-implant tissues after implant placement is necessary and will dictate the need for additional surgical procedures during the uncovering surgery, prosthetic phase or maintenance care. In this context, CBCT use may become limited since implant artifacts such as scattering and blooming can prevent a clear view of the peri-implant tissues, especially in situations where a thin bony wall is encountered (Razavi, Palmer, Davies, Wilson, & Palmer, 2010; Vanderstuyft et al., 2019). Inferior image resolution around implants could undermine the value of CBCT, rendering inappropriate treatment. Additionally, repeated radiation exposures as well as the added cost constraint its routine use for monitoring peri-implant bone loss. On the other hand, US could clearly delineate soft and hard-tissue around implants, allowing for linear/area quantifications without radiation and artifact concerns. Both imaging modalities should be used hand in hand to provide the most optimal care to patients in need of implant rehabilitation.

In light of the differences in the mode of action and advantages/disadvantages of both imaging modalities summarized in Table 1, it becomes natural to combine them for delivering efficient and synergistic diagnostic values. CBCT is a great tool to provide general 3-dimensional anatomical information in a large field of view, for example, single or both jaws with clinically acceptable accuracy (~150–500 μm). During implant treatment phase, CBCT is becoming a part of standard care for comprehensive evaluation of relevant anatomical structures, especially for full mouth reconstruction. Although there is insufficient evidence to recommend CBCT as a standard diagnostic tool for assessment of peri-implant bone loss (Pelekos et al., 2018), a recent experimental study demonstrated an average underestimation of <1 mm on measurements for height and width of peri-implant defects (Schriber et al., 2020). The authors of the latter study highlighted that the precision of linear measurements can be impaired due to diameter, CBCT device and more importantly the implant material and observer background resulting mostly in an underestimation of the defect dimensions (Schriber et al., 2020). Meanwhile, US imaging emerges as a novel and high-resolution (~60 μm) modality to aid in peri-implant tissue evaluation and monitoring without artifact interference. Previous efforts by our group (Barootchi et al., 2020; Chan & Kripfgans, 2020; Chan et al., 2017,

2018; Tattan et al., 2019) demonstrate US as a promising modality to image intraoral hard and soft tissues and important vital structures, for example, the mental foramen, greater palatine foramen and lingual nerve. However, US has its own disadvantages, including the need for a medium for sound conduction, the inability to penetrate into bone, a narrow field of view and a learning curve required to adapt to this new technology.

Limitations of this study include small sample size, measurement variability and a lack of standardized spatial measurement locations. Nevertheless, this preliminary study showed agreement of US measurements with CBCT and direct measurements, demonstrating the feasibility of US to evaluate and monitor peri-implant tissue dimensions and change and confirming the hypothesis of the present pilot study. Furthermore, functional analysis of peri-implant soft tissues brought about by the US (e.g., tissue density and blood flow) may shed light on quantitative evaluation of peri-implant inflammation and soft-tissue destruction. After confirmation, this could possibly improve the current clinical method of diagnosing peri-implant tissue inflammation such as tissue color examination and bleeding on probing. However, clinical trials with appropriate sample size is necessary to confirm the findings of this pilot study.

5 | CONCLUSION

Currently, non-invasive and 3-dimensional evaluation of peri-implant hard and soft tissues is much needed for accurate diagnosis and outcome evaluation of peri-implant diseases and conditions. Preliminary data demonstrated feasibility of US in measuring facial bone level and thickness on humans through comparison with CBCT and clinical photography measurements. US can be especially useful in cases with thin facial bone or when CBCT imaging quality may be hindered by artifacts. Additional features, including the color imaging and soft-tissue pixel brightness, make US very attractive to complement CBCT and clinical examination for improving diagnostic capability.

AUTHOR CONTRIBUTION

Rafael Siqueira: Data curation (equal); Resources (equal); Writing-original draft (equal); Writing-review & editing (equal). **Khaled Sinjab:** Data curation (equal); Resources (equal); Visualization (equal). **Ying-Chun Pan:** Data curation (equal); Formal analysis (equal); Resources (equal); Software (equal); Validation (equal); Writing-original draft (equal); Writing-review & editing (equal). **Fabiana Soki:** Data curation

(equal); Formal analysis (equal); Software (equal); Supervision (equal); Validation (equal); Writing-original draft (equal); Writing-review & editing (equal). **Hsun-Liang Chan:** Conceptualization (lead); Data curation (equal); Formal analysis (equal); Funding acquisition (lead); Investigation (lead); Methodology (lead); Resources (lead); Software (equal); Supervision (lead); Validation (lead); Visualization (equal); Writing-original draft (lead); Writing-review & editing (lead). **Oliver Kripfgans:** Conceptualization (equal); Data curation (equal); Formal analysis (equal); Funding acquisition (equal); Investigation (equal); Methodology (equal); Resources (equal); Software (equal); Supervision (equal); Validation (equal); Visualization (equal); Writing-original draft (equal); Writing-review & editing (equal).

ORCID

Rafael Siqueira https://orcid.org/0000-0003-4081-0959
Khaled Sinjab https://orcid.org/0000-0002-4570-9385
Ying-Chun Pan https://orcid.org/0000-0003-2602-592X
Hsun-Liang Chan https://orcid.org/0000-0001-5952-0447
Oliver Kripfgans https://orcid.org/0000-0003-2905-1496

REFERENCES

Adler, L., Buhlin, K., & Jansson, L. (2020). Survival and complications: A 9- to 15-year retrospective follow-up of dental implant therapy. *Journal of Oral Rehabilitation*, *47*(1), 67–77. https://doi.org/10.1111/joor.12866

Barootchi, S., Chan, H. L., Namazi, S. S., Wang, H. L., & Kripfgans, O. D. (2020). Ultrasonographic characterization of lingual structures pertinent to oral, periodontal, and implant surgery. *Clinical Oral Implants Research*, *31*(4), 352–359. https://doi.org/10.1111/clr.13573

Berglundh, T., Armitage, G., Araujo, M. G., Avila-Ortiz, G., Blanco, J., Camargo, P. M., & Zitzmann, N. (2018). Peri-implant diseases and conditions: Consensus report of workgroup 4 of the 2017 world workshop on the classification of periodontal and peri-implant diseases and conditions. *Journal of Periodontology*, *89*(Suppl 1), S313–S318. https://doi.org/10.1002/JPER.17-0739

Bornstein, M. M., Scarfe, W. C., Vaughn, V. M., & Jacobs, R. (2014). Cone beam computed tomography in implant dentistry: A systematic review focusing on guidelines, indications, and radiation dose risks. *International Journal of Oral and Maxillofacial Implants*, *29*(Suppl), 55–77. https://doi.org/10.11607/jomi.2014suppl.g1.4

Chan, H. L., & Kripfgans, O. D. (2020). Ultrasonography for diagnosis of peri-implant diseases and conditions: A detailed scanning protocol and case demonstration. *Dentomaxillofacial Radiology*, *49*(7), 20190445, https://doi.org/10.1259/dmfr.20190445

Chan, H. L., Misch, K., & Wang, H. L. (2010). Dental imaging in implant treatment planning. *Implant Dentistry*, *19*(4), 288–298. https://doi.org/10.1097/ID.0b013e3181e59ebd

Chan, H. L., Sinjab, K., Chung, M. P., Chiang, Y. C., Wang, H. L., Giannobile, W. V., & Kripfgans, O. D. (2017). Non-invasive evaluation of facial crestal bone with ultrasonography. *PLoS One*, *12*(2), e0171237. https://doi.org/10.1371/journal.pone.0171237

Chan, H. L., Sinjab, K., Li, J., Chen, Z., Wang, H. L., & Kripfgans, O. D. (2018). Ultrasonography for noninvasive and real-time evaluation of peri-implant tissue dimensions. *Journal of Clinical Periodontology*, *45*(8), 986–995. https://doi.org/10.1111/jcpe.12918

de Siqueira, R. A. C., Savaget Gonçalves Junior, R, Santos, P. G. F, Mattias Sartori, I. A, Wang, H. L, & Fontão, F. N. G. K (2020). Effect of different implant placement depths on crestal bone levels and soft tissue behavior: A 5-year randomized clinical trial. *Clin Oral Implants Res*, *31*(3), 282–293. https://doi.org/10.1111/clr.13569

de Azevedo-Vaz, S. L, Peyneau, P. D, Ramirez-Sotelo, L. R, Vasconcelos, K. F, Campos, P. S. F, & Haiter-Neto, F (2016). Efficacy of a cone beam computed tomography metal artifact reduction algorithm for the detection of peri-implant fenestrations and dehiscences. *Oral Surgery, Oral Medicine, Oral Pathology and Oral Radiology*, *121*(5), 550–556. https://doi.org/10.1016/j.oooo.2016.01.013

Demirturk Kocasarac, H., Ustaoglu, G., Bayrak, S., Katkar, R., Geha, H., Deahl, S. T. 2nd, & Noujeim, M. (2019). Evaluation of artifacts generated by titanium, zirconium, and titanium-zirconium alloy dental implants on MRI, CT, and CBCT images: A phantom study. *Oral Surgery, Oral Medicine, Oral Pathology and Oral Radiology*, *127*(6), 535–544. https://doi.org/10.1016/j.oooo.2019.01.074

Dietrich, C. F., Sirlin, C. B., O'Boyle, M., Donga, Y., & Jenssen, C. (2019). Editorial on the current role of ultrasound. *Applied Sciences*, *9*(3512), 9. https://doi.org/10.3390/app9173512

Fu, J. H., Yeh, C. Y., Chan, H. L., Tatarakis, N., Leong, D. J., & Wang, H. L. (2010). Tissue biotype and its relation to the underlying bone morphology. *Journal of Periodontology*, *81*(4), 569–574. https://doi.org/10.1902/jop.2009.090591

Horner, K., O'Malley, L., Taylor, K., & Glenny, A. M. (2015). Guidelines for clinical use of CBCT: A review. *Dentomaxillofacial Radiology*, *44*(1), 20140225. https://doi.org/10.1259/dmfr.20140225

Jacobs, R., Vranckx, M., Vanderstuyft, T., Quirynen, M., & Salmon, B. (2018). CBCT vs other imaging modalities to assess peri-implant bone and diagnose complications: A systematic review. *European Journal of Oral Implantology*, *11*(Suppl 1), 77–92.

Linkevicius, T., Apse, P., Grybauskas, S., & Puisys, A. (2009). The influence of soft tissue thickness on crestal bone changes around implants: A 1-year prospective controlled clinical trial. *International Journal of Oral and Maxillofacial Implants*, *24*(4), 712–719.

Linkevicius, T., Linkevicius, R., Alkimavicius, J., Linkeviciene, L., Andrijauskas, P., & Puisys, A. (2018). Influence of titanium base, lithium disilicate restoration and vertical soft tissue thickness on bone stability around triangular-shaped implants: A prospective clinical trial. *Clinical Oral Implants Research*, *29*(7), 716–724. https://doi.org/10.1111/clr.13263

Linkevicius, T., Puisys, A., Steigmann, M., Vindasiute, E., & Linkeviciene, L. (2015). Influence of vertical soft tissue thickness on crestal bone changes around implants with platform switching: A comparative clinical study. *Clinical Implant Dentistry and Related Research*, *17*(6), 1228–1236. https://doi.org/10.1111/cid.12222

Monje, A., Chappuis, V., Monje, F., Munoz, F., Wang, H. L., Urban, I. A., & Buser, D. (2019). The critical peri-implant buccal bone wall thickness revisited: An experimental study in the beagle dog. *International Journal of Oral and Maxillofacial Implants*, *34*(6), 1328–1336. https://doi.org/10.11607/jomi.7657

Monje, A., Pons, R., Insua, A., Nart, J., Wang, H. L., & Schwarz, F. (2019). Morphology and severity of peri-implantitis bone defects. *Clinical Implant Dentistry and Related Research*, *21*(4), 635–643. https://doi.org/10.1111/cid.12791

Moraschini, V., Poubel, L. A., Ferreira, V. F., & Barboza Edos, S. (2015). Evaluation of survival and success rates of dental implants reported in longitudinal studies with a follow-up period of at least 10 years: A systematic review. *International Journal of Oral and Maxillofacial Surgery*, *44*(3), 377–388. https://doi.org/10.1016/j.ijom.2014.10.023

Pauwels, R, Stamatakis, H, Bosmans, H, Bogaerts, R, Jacobs, R, Horner, K, & Tsiklakis, K (2013). Quantification of metal artifacts on cone beam computed tomography images. *Clinical Oral Implants Research*, *24*(Suppl A100), 94–99. https://doi.org/10.1111/j.1600-0501.2011.02382.x

Pelekos, G., Acharya, A., Tonetti, M. S., & Bornstein, M. M. (2018). Diagnostic performance of cone beam computed tomography in assessing peri-implant bone loss: A systematic review. *Clinical Oral Implants Research*, *29*(5), 443–464. https://doi.org/10.1111/clr.13143

Perussolo, J., Souza, A. B., Matarazzo, F., Oliveira, R. P., & Araujo, M. G. (2018). Influence of the keratinized mucosa on the stability of peri-implant tissues and brushing discomfort: A 4-year follow-up study. *Clinical Oral Implants Research*, *29*(12), 1177–1185. https://doi.org/10.1111/clr.13381

Peterson, A. G., Wang, M., Gonzalez, S., Covell, D. A. Jr, Katancik, J., & Sehgal, H. S. (2018). An In vivo and cone beam computed tomography investigation of the accuracy in measuring alveolar bone height and detecting dehiscence and fenestration defects. *International Journal of Oral and Maxillofacial Implants*, *33*(6), 1296–1304. https://doi.org/10.11607/jomi.6633

Razavi, T., Palmer, R. M., Davies, J., Wilson, R., & Palmer, P. J. (2010). Accuracy of measuring the cortical bone thickness adjacent to dental implants using cone beam computed tomography. *Clinical Oral Implants Research*, *21*(7), 718–725. https://doi.org/10.1111/j.1600-0501.2009.01905.x

Renvert, S., Persson, G. R., Pirih, F. Q., & Camargo, P. M. (2018). Peri-implant health, peri-implant mucositis, and peri-implantitis: Case definitions and diagnostic considerations. *Journal of Periodontology*, *89*(Suppl 1), S304–S312. https://doi.org/10.1002/JPER.17-0588

Rios, H. F., Borgnakke, W. S., & Benavides, E. (2017). The use of cone-beam computed tomography in management of patients requiring dental implants: An american academy of periodontology best evidence review. *Journal of Periodontology*, *88*(10), 946–959. https://doi.org/10.1902/jop.2017.160548

Schriber, M., Yeung, A. W. K., Suter, V. G. A., Buser, D., Leung, Y. Y., & Bornstein, M. M. (2020). Cone beam computed tomography artefacts around dental implants with different materials influencing the detection of peri-implant bone defects. *Clinical Oral Implants Research*, *31*(7), 595–606. https://doi.org/10.1111/clr.13596

Schulze, R. K., Berndt, D., & d'Hoedt, B. (2010). On cone-beam computed tomography artifacts induced by titanium implants. *Clinical Oral Implants Research*, *21*(1), 100–107. https://doi.org/10.1111/j.1600-0501.2009.01817.x

Schulze, R., Heil, U., Gross, D., Bruellmann, D. D., Dranischnikow, E., Schwanecke, U., & Schoemer, E. (2011). Artefacts in CBCT: A review. *Dentomaxillofacial Radiology*, *40*(5), 265–273. https://doi.org/10.1259/dmfr/30642039

Schwarz, F., Becker, J., Civale, S., Sahin, D., Iglhaut, T., & Iglhaut, G. (2018). Influence of the width of keratinized tissue on the development and resolution of experimental peri-implant mucositis lesions in humans. *Clinical Oral Implants Research*, *29*(6), 576–582. https://doi.org/10.1111/clr.13155

Schwarz, F., Derks, J., Monje, A., & Wang, H. L. (2018). Peri-implantitis. *Journal of Periodontology*, *89*(Suppl 1), S267–S290. https://doi.org/10.1002/JPER.16-0350

Schwarz, F., Herten, M., Sager, M., Bieling, K., Sculean, A., & Becker, J. (2007). Comparison of naturally occurring and ligature-induced peri-implantitis bone defects in humans and dogs.

Clinical Oral Implants Research, *18*(2), 161–170. https://doi.org/10.1111/j.1600-0501.2006.01320.x

Spray, J. R., Black, C. G., Morris, H. F., & Ochi, S. (2000). The influence of bone thickness on facial marginal bone response: Stage 1 placement through stage 2 uncovering. *Annals of Periodontology*, *5*(1), 119–128. https://doi.org/10.1902/annals.2000.5.1.119

Tattan, M., Sinjab, K., Lee, E., Arnett, M., Oh, T. J., Wang, H. L., & Kripfgans, O. D. (2019). Ultrasonography for chairside evaluation of periodontal structures: A pilot study. *Journal of Periodontology*, https://doi.org/10.1002/JPER.19-0342

Thoma, D. S., Gasser, T. J. W., Jung, R. E., & Hammerle, C. H. F. (2020). Randomized controlled clinical trial comparing implant sites augmented with a volume-stable collagen matrix or an autogenous connective tissue graft: 3-year data after insertion of reconstructions. *Journal of Clinical Periodontology*, https://doi.org/10.1111/jcpe.13271

Tyndall, D. A., Price, J. B., Tetradis, S., Ganz, S. D., Hildebolt, C., Scarfe, W. C., & Maxillofacial, R. (2012). Position statement of the American Academy of Oral and Maxillofacial Radiology on selection criteria for the use of radiology in dental implantology with emphasis on cone beam computed tomography. *Oral Surgery, Oral Medicine, Oral Pathology and Oral Radiology*, *113*(6), 817–826. https://doi.org/10.1016/j.oooo.2012.03.005

van Eekeren, P., van Elsas, P., Tahmaseb, A., & Wismeijer, D. (2017). The influence of initial mucosal thickness on crestal bone change in similar macrogeometrical implants: A prospective randomized clinical trial. *Clinical Oral Implants Research*, *28*(2), 214–218. https://doi.org/10.1111/clr.12784

Vanderstuyft, T., Tarce, M., Sanaan, B., Jacobs, R., de Faria Vasconcelos, K., & Quirynen, M. (2019). Inaccuracy of buccal bone thickness estimation on cone-beam CT due to implant blooming: An ex-vivo study. *Journal of Clinical Periodontology*, *46*(11), 1134–1143. https://doi.org/10.1111/jcpe.13183

Vervaeke, S., Matthys, C., Nassar, R., Christiaens, V., Cosyn, J., & De Bruyn, H. (2018). Adapting the vertical position of implants with a conical connection in relation to soft tissue thickness prevents early implant surface exposure: A 2-year prospective intra-subject comparison. *Journal of Clinical Periodontology*, *45*(5), 605–612. https://doi.org/10.1111/jcpe.12871

SUPPORTING INFORMATION

Additional supporting information may be found online in the Supporting Information section.

How to cite this article: Siqueira R, Sinjab K, Pan Y-C, Soki F, Chan H-L, Kripfgans O. Comprehensive peri-implant tissue evaluation with ultrasonography and cone-beam computed tomography: A pilot study. *Clin Oral Impl Res*. 2021;32:777–785. https://doi.org/10.1111/clr.13758